Interaction of Inhibitors of the Vacuolar H^+-ATPase with the Transmembrane V_o-Sector†

Tibor Páli,[‡,§] Graham Whyteside,[||,⊥] Neil Dixon,[@] Terence P. Kee,[@] Stephen Ball,[@] Michael A. Harrison,[@] John B. C. Findlay,[@] Malcolm E. Finbow,[||] and Derek Marsh*[,‡]

Max-Planck-Institut für biophysikalische Chemie, Abt. Spektroskopie, 37070 Göttingen, Germany, Chemistry Department and School of Biochemistry and Molecular Biology, University of Leeds, Leeds LS2 9JT, U.K., and Department of Biological and Biomedical Sciences, Glasgow Caledonian University, Glasgow G4 0BA, U.K.

Received March 30, 2004; Revised Manuscript Received May 26, 2004

ABSTRACT: The macrolide antibiotic concanamycin A and a designed derivative of 5-(2-indolyl)-2,4-pentadienamide (INDOL0) are potent inhibitors of vacuolar H^+-ATPases, with IC_{50} values in the low and medium nanomolar range, respectively. Interaction of these V-ATPase inhibitors with spin-labeled subunit *c* in the transmembrane V_o-sector of the ATPase was studied by using the transport-active 16-kDa proteolipid analogue of subunit *c* from the hepatopancreas of *Nephrops norvegicus*. Analogous experiments were also performed with vacuolar membranes from *Saccharomyces cerevisiae*. Membranous preparations of the *Nephrops* 16-kDa proteolipid were spin-labeled either on the unique cysteine C54, with a nitroxyl maleimide, or on the functionally essential glutamate E140, with a nitroxyl analogue of dicyclohexylcarbodiimide (DCCD). These residues were previously demonstrated to be accessible to lipid. Interaction of the inhibitors with these lipid-exposed residues was studied by using both conventional and saturation transfer EPR spectroscopy. Immobilization of the spin-labeled residues by the inhibitors was observed on both the nanosecond and microsecond time scales. The perturbation by INDOL0 was mostly greater than that by concanamycin A. Qualitatively similar but quantitatively greater effects were obtained with the same spin-label reagents and vacuolar membranes in which the *Nephrops* 16-kDa proteolipid was expressed in place of the native vma3p proteolipid of yeast. The spin-label immobilization corresponds to a direct interaction of the inhibitors with these intramembranous sites on the protein. A mutational analysis on transmembrane segment 4 known to give resistance to concanamycin A also gave partial resistance to INDOL0. The results are consistent with transmembrane segments 2 and 4 of the 16-kDa putative four-helix bundle, and particularly the functionally essential protonation locus, being involved in the inhibitor binding sites. Inhibition of proton transport may also involve immobilization of the overall rotation of the proteolipid subunit assembly.

The vacuolar H^+-ATPases are proton pumps that are involved in the acidification of intracellular compartments (endosomes, lysosomes, vacuoles, and vesicles) and, in the case of the osteoclast, of the extracellular lacunae at the surface of the resorbing bone (*1*, *2*). Proton translocation through the transmembrane V_o-sector of the protein (see Figure 1) is mediated by a glutamic acid residue in the 16-kDa proteolipid *c* subunit. Transport is blocked when this residue is covalently modified with dicyclohexylcarbodiimide (DCCD).[1] The 16-kDa proteolipid that is isolated from the hepatopancreas of the lobster *Nephrops norvegicus* is able to substitute functionally for the *c* subunit in yeast, producing a hybrid V-ATPase that is sensitive to DCCD (*3*, *4*). Membranous preparations of the 16-kDa proteolipid can be isolated from *Nephrops* as hexameric assemblies, and have been used extensively for biophysical studies of subunit *c*, in the absence of other components of the V_o-sector (*5*−*7*).

The V_o-sector of the ATPase is a potential therapeutic target because of the direct involvement of the osteoclast V-ATPase in the excessive bone resorption that is associated with osteoporosis. Possible synthetic strategies are based on the macrolide antibiotics concanamycin and bafilomycin which are specific inhibitors of the V-ATPases, but have little effect on F-ATPases and inhibit P-type ATPases only

† This work was supported by Contract QLG-CT-2000-01801 of the European Commission.

* To whom correspondence should be addressed: Max-Planck-Institut für biophysikalische Chemie, Abt. Spektroskopie, 37070 Göttingen, Germany. Telephone: +49-551 201 1285. Fax: +49-551 201 1501. E-mail: dmarsh@gwdg.de.

‡ Max-Planck-Institut für biophysikalische Chemie.

§ Permanent address: Institute of Biophysics, Biological Research Centre, H-6701 Szeged, Hungary.

|| Glasgow Caledonian University.

⊥ Present address: School of Biochemistry and Molecular Biology, University of Leeds, Leeds LS2 9JT, U.K.

@ University of Leeds.

[1] Abbreviations: V-ATPase, vacuolar H^+-ATPase; INDOL0, 5-(5,6-dichloro-2-indolyl)-2-methoxy-*N*-(1,2,2,6,6-pentamethylpiperidin-4-yl)-2,4-pentadienamide; 5-MSL, 3-maleimido-2,2,5,5-tetramethylpyrrolidine-*N*-oxyl; DCCD, *N*,*N*′-dicyclohexylcarbodiimide; NCCD, *N*-(2,2,6,6-tetramethylpiperidine-1-oxy)-*N*′-cyclohexylcarbodiimide; DMSO, dimethyl sulfoxide; EPR, electron paramagnetic resonance; ST-EPR, saturation transfer EPR; V_1, first-harmonic absorption EPR spectrum detected in phase with respect to the static magnetic field modulation; V_2', second-harmonic absorption EPR spectrum detected 90° out of phase with respect to the static magnetic field modulation.

10.1021/bi0493867 CCC: $27.50
Published on Web 09/01/2004

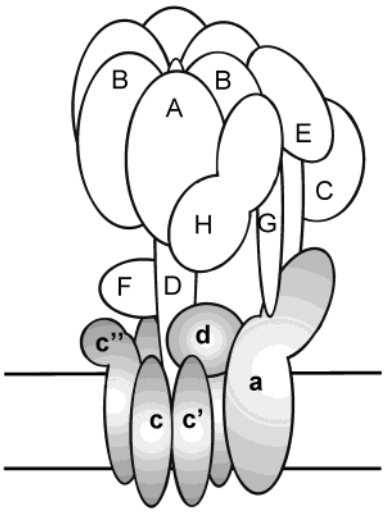

FIGURE 1: Schematic arrangement of the subunits in V-ATPases consistent with current data on protein−protein interactions. The transmembrane V_o-sector is shaded gray. Proteolipid subunit *c* is *vma3p* (at least four copies) in yeast; *c′* is *vma11p* (one copy), and *c″* is *vma16p* (one copy). Subunit *a* is the large *vph1p* polypeptide in yeast, and *d* is *vma6p*. Within the membrane, *c*, *c′*, and *c″* belong to the rotor assembly and *a* belongs to the stator of the rotary motor.

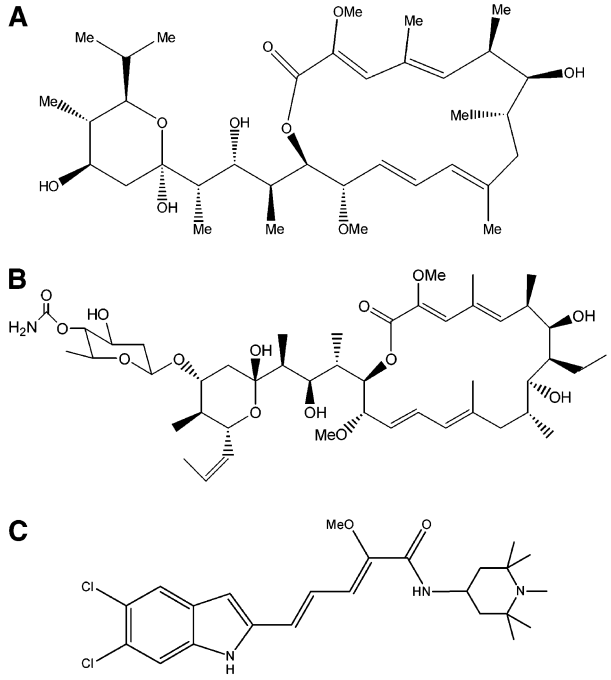

FIGURE 2: (A) Bafilomycin A_1, (B) concanamycin A, and (C) 5-(5,6-dichloro-2-indolyl)-2-methoxy-*N*-(1,2,2,6,6-pentamethylpiperidin-4-yl)-2,4-pentadienamide (INDOL0).

at much higher concentrations (*8*, *9*). Structure−activity analyses (*10*, *11*) have led to the development of the 5-(5,6-dichloro-2-indolyl)-2-methoxy-2,4-pentadienamide family of inhibitors as possible lead compounds (*12*). One of the most potent discovered so far is the 1,2,2,6,6-pentamethylpiperidin-4-yl derivative, INDOL0 (see Figure 2), which has an IC_{50} of 29 nM in chicken osteoclasts, and exhibits a selectivity for the osteoclast enzyme over other V-ATPases (*13*).

In this work, we study the interaction of concanamycin A and the synthetic indolyl inhibitor INDOL0 with the 16-kDa proteolipid from *Nephrops* that has been spin-labeled specifically either on the functionally essential glutamic acid residue (E140) or on the unique cysteine residue (C54). The intramembranous location of these spin-labeled residues has been investigated previously by us (*5*). Conventional and saturation transfer (ST) EPR spectroscopy are used to characterize perturbations by the inhibitors of both the local and overall rotational mobility of the protein. Parallel experiments, using the same selective spin-labeling reagents, are performed with yeast vacuolar membranes in which the native *c* subunit that is encoded by the *VMA3* gene is replaced by recombinant 16-kDa *Nephrops* proteolipid. Known mutations (*14*) of the 16-kDa proteolipid are used to verify a common binding site for the inhibitors concanamycin A, bafilomycin, and INDOL0.

EXPERIMENTAL PROCEDURES

Materials. Concanamycin A was obtained from Fluka (Buchs, Switzerland). The 5-(5,6-dichloro-2-indolyl)-2,4-pentadienoyl inhibitor INDOL0 was synthesized according to the methods of refs *10* and *13*. Spin-labeled maleimide (5-MSL) was obtained from Syva (Palo Alto, CA), and the spin-labeled DCCD derivative (NCCD) was prepared according to the methods of refs *15* and *16*. The W303-1B vatc cells (*MAT*α *ade2, ura3, leu2 his3, trp1,* Δ*vma3::LEU2*) were a kind gift of Y. Anraku (*3*).

Isolation of 16-kDa Membranes and Vacuolar Membranes. Membranes containing the 16-kDa channel proteolipid were prepared from the hepatopancreas of the decapod *N. norvegicus* by extraction with 20 mM NaOH according to the procedure of refs *17* and *18*, as described previously (*7*). Expression of the *Nephrops* 16-kDa proteolipid in *Saccharomyces cerevisiae* W303-1B vatc strain, in which the endogeneous *VMA3* gene had been inactivated, was performed as described previously (*3*, *4*). EDTA-washed yeast vacuolar membranes were prepared as described in ref *19*.

Spin Labeling. Membranes were suspended in 50 mM Hepes buffer, with 10 mM NaCl and 10 mM EDTA (pH 7.8). Covalent spin labeling of *Nephrops* 16-kDa membranes with 5-MSL or NCCD was performed and characterized as described previously (*7*). Typically, membranes (ca. 1 mg of membrane protein) in 8 mL of buffer were reacted with 2 mM 5-MSL added in buffer or with 250 μM NCCD added from a concentrated solution in ethanol. Spin labeling of yeast vacuolar membranes with the same covalent reagents was performed in a similar manner, except that half the quantities were used in the same volume of buffer. Inhibitors were added to a final concentration of 125 μM from solutions in 50 μL of DMSO, which corresponds to a nominal 1:1 inhibitor:lipid mole ratio for 16-kDa membranes. An equal volume of DMSO was added to the control samples. After being washed to remove excess spin labeling reagent, membranes were packed in 1 mm inside-diameter glass capillaries by pelleting in a benchtop centrifuge. The sample length was trimmed to 5 mm; excess supernatant was removed, and the capillary was flame-sealed.

EPR Spectroscopy. EPR spectra were recorded on a Varian Century-Line 9 GHz spectrometer with 100 kHz field modulation. Sample capillaries were accommodated in standard quartz EPR tubes that contained light silicone oil for thermal stability. The temperature was regulated by a thermostated nitrogen gas flow, and measured with a fine-wire thermocouple situated in the silicone oil at the top of the microwave cavity. The 5 mm sample was centered in

the rectangular TE_{102} resonator to minimize microwave- and modulation-field inhomogeneities (*20*). The microwave H_1 field at the sample was measured as described in the latter reference. Conventional EPR spectra were recorded in the in-phase first-harmonic absorption mode (V_1 display) and ST-EPR spectra in the out-of-phase second-harmonic absorption mode (V_2' display) (see ref *21*). Effective rotational correlation times were obtained from ST-EPR spectra by using calibrations with spin-labeled hemoglobin in solutions of known viscosity (*22*) that are given in ref *23*.

Construction of Mutations in the S. cerevisiae Form of the 16-kDa Proteolipid. Single mutants F135L and Y142H were created using a PCR-based strategy provided by Stratagene (Quikchange site-directed mutagenesis kit), according to the manufacturer's instructions. The wild-type gene had previously been tagged at the 3′ end with the HA1 epitope (*24*) in the p424 ADH shuttle vector, and was used as a template. The PCR products were cloned into the p424 ADH vector and sequenced, which showed no changes other than the desired mutation. The inserted gene in this vector is constitutively transcribed.

Measurement of V-ATPase Activity. W303-1B vatc cells were transfected with the wild type and various mutant forms of the 16-kDa proteolipid. Cells were grown in minimal medium supplemented with the nutrients required to maintain the presence of the p424 vector. Vacuoles were prepared for measurement of ATPase activity as previously described (*24*).

RESULTS AND DISCUSSION

Membranous preparations of the 16-kDa proteolipid subunit from *Nephrops* were spin-labeled specifically either on residue C54 with 5-MSL or on residue E140 with NCCD. The effect of the two inhibitors, concanamycin A and INDOL0, on the rotational mobility of these spin-labeled side chains was studied. Corresponding experiments, with the same spin labeling reagents, were performed on yeast vacuolar membranes in which the endogeneous subunit *c* of the V-ATPase was replaced by the *Nephrops* 16-kDa proteolipid. Complementary mutational analysis of transmembrane segment 4 was used to further probe the inhibitory sites.

Nephrops 16-kDa Proteolipid Membranes. The top panel of Figure 3 shows the conventional V_1-EPR spectra of alkali-extracted 16-kDa proteolipid membranes covalently spin-labeled with the maleimide nitroxide, 5-MSL. Spectra are shown for samples in the presence and absence of inhibitors. As found previously (*7*), the spectra consist predominantly of a strongly immobilized component with outer hyperfine splitting, $2A_{max}$, that approaches the rigid limit. An additional sharp three-line component is prominent in the first-derivative spectra at 35 °C, but this contributes relatively little to the total double-integrated spectral intensity. These qualitative spectral features remain unchanged in the presence of the two inhibitors. In part, this may be attributed to the fact that the principal spectral component lies in the slow motional regime, where the spectra are less sensitive to changes in rotational mobility of the spin label.

Figure 4A gives the temperature dependence of the outer hyperfine splitting, $2A_{max}$, of 5-MSL, for the *Nephrops* 16-kDa membranes in the presence and absence of the

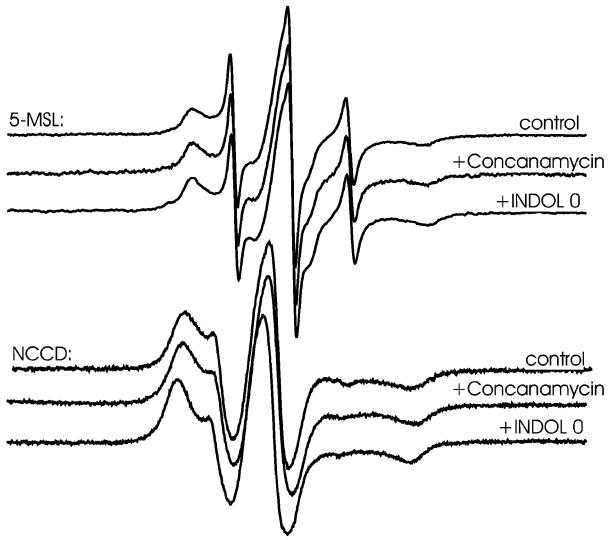

FIGURE 3: Conventional EPR spectra (V_1-display) of the 5-MSL (top panel) and NCCD (bottom panel) spin labels covalently bound to alkaline-extracted membranes of the *Nephrops* 16-kDa proteolipid. For each set of spectra: (top) control sample (to which DMSO was added); (middle) sample containing concanamycin A; (bottom) sample containing INDOL0. Temperature 35 °C; total scan width was 160 gauss.

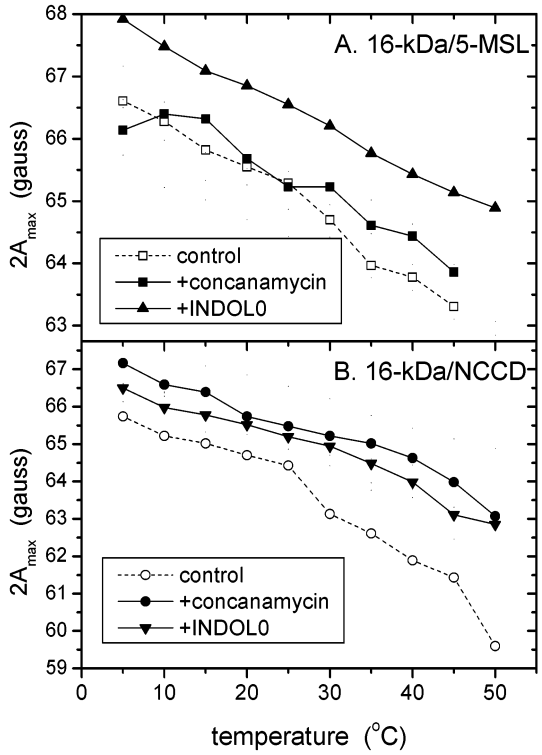

FIGURE 4: Temperature dependence of the outer hyperfine splitting, $2A_{max}$, for alkaline-extracted 16-kDa membranes spin-labeled with either (A) 5-MSL or (B) NCCD, as indicated. Note the difference in ordinate between panels A and B: (□ and ○) control samples, (■ and ●) samples with concanamycin A added, and (▲ and ▼) samples with INDOL0 added.

inhibitors. The characteristic increase in rotational mobility of the spin label with increase in temperature is seen from the progressively decreasing values of $2A_{max}$. Concanamycin A increases the outer splitting of the spin-labeled C54 side chain, at temperatures of ≥30 °C. At lower temperatures, the effect of concanamycin A is smaller. INDOL0, added at the same molar concentration, produces a larger perturbation

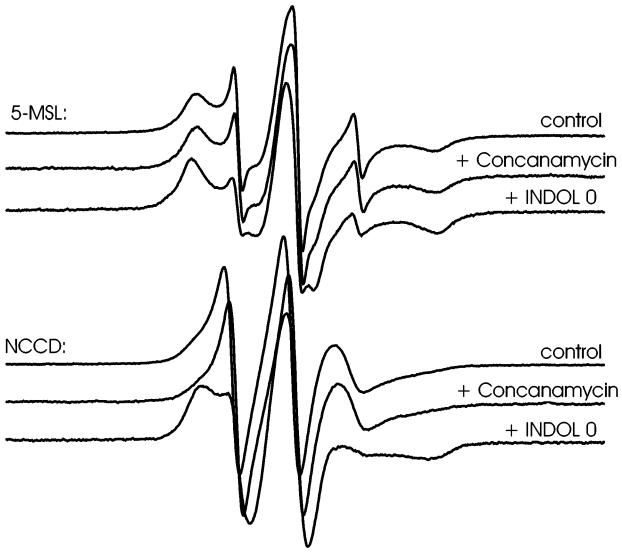

FIGURE 5: Conventional EPR spectra (V_1-display) of the 5-MSL (top panel) and NCCD (bottom panel) spin labels covalently bound to yeast vacuolar membranes. For each set of spectra: (top) control sample (to which DMSO was added); (middle) sample containing concanamycin A; (bottom) sample containing INDOL0. Temperature 35 °C; total scan width was 160 G.

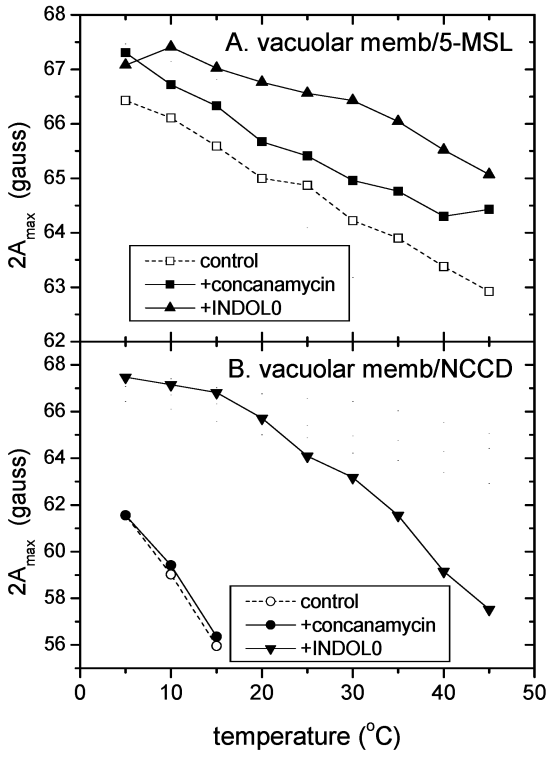

FIGURE 6: Temperature dependence of the outer hyperfine splitting, $2A_{max}$, for yeast vacuolar membranes spin-labeled with either (A) 5-MSL or (B) NCCD, as indicated. Note the difference in ordinate between panels A and B: (□ and ○) control samples, (■ and ●) samples with concanamycin A added, and (▲ and ▼) samples with INDOL0 added.

than does concanamycin A. The values of $2A_{max}$ are consistently larger in the presence of INDOL0 than in the presence of concanamycin A. Thus, both inhibitors interact with the spin-labeled C54 residue by reducing its segmental rotational mobility, but INDOL0 to a greater extent than concanamycin A.

The bottom panel of Figure 3 shows the conventional V_1-EPR spectra of *Nephrops* 16-kDa membranes covalently spin-labeled with NCCD, the nitroxide derivative of DCCD. Again, spectra are shown in the presence and absence of inhibitors. In this case, the spectra evidence increased mobility relative to those of 5-MSL. For the control membranes, there is significant motional narrowing of the spectral anisotropy at 35 °C; the outer hyperfine splitting no longer approaches so closely to the rigid limit. In the presence of INDOL0 or concanamycin, the spin label on glutamic acid E140 is more strongly immobilized, which indicates a perturbation arising from direct interaction with the indolyl inhibitor. Photolabeling of V-ATPase subunit *c* by a concanamycin derivative has been demonstrated previously (*25*).

The temperature dependence of the outer hyperfine splitting of the NCCD label bound to *Nephrops* 16-kDa membranes is given in Figure 4B. Concanamycin A shows a greater perturbation of the mobility of spin-labeled E140 than of spin-labeled C54. (Note the difference in ordinate scales between panels A and B of Figure 4.) Also, the effect of concanamycin A slightly exceeds that of INDOL0, which is the reverse of the situation for spin-labeled C54.

Yeast Vacuolar Membranes. The top panel of Figure 5 shows the conventional V_1-EPR spectra of yeast vacuolar membranes that are spin-labeled with 5-MSL. Qualitatively, the spectra are rather similar to those of the *Nephrops* 16-kDa proteolipid also spin-labeled with 5-MSL. Figure 6A gives the temperature dependence of the outer hyperfine splitting of 5-MSL for vacuolar membranes in the presence and absence of inhibitors. For control membranes, the temperature dependence is similar to that for *Nephrops* 16-kDa membranes, although the absolute values of $2A_{max}$ are slightly smaller. Concanamycin A induces an increase in $2A_{max}$ throughout the entire temperature range. The perturbation of the spin-label mobility by INDOL0 is again greater than that by concanamycin A, and slightly larger than that in *Nephrops* 16-kDa membranes. Overall, the effects of the two inhibitors are rather similar in both membrane systems.

The bottom panel of Figure 5 shows the conventional V_1-EPR spectra of yeast vacuolar membranes spin-labeled with NCCD. Studies with a fluorescent analogue of DCCD have shown that Glu140 of the 16-kDa proteolipid is the only site that is labeled appreciably in vacuolar membranes (*26*). The NCCD spectra of control membranes and those in the presence of concanamycin are extensively motionally narrowed at 35 °C. In contrast, the spectra from membranes to which INDOL0 is added are still appreciably motionally restricted. Figure 6B gives the temperature dependence of the outer hyperfine splitting of NCCD for vacuolar membranes in the presence and absence of inhibitors. The effect of concanamycin is slight. The outer hyperfine peaks are resolved only up to 15 °C, for both control membranes and those in the presence of concanamycin A. INDOL0 causes a large increase in the value of $2A_{max}$ for NCCD-labeled vacuolar membranes. The outer hyperfine peaks remain resolved up to 45 °C in the presence of INDOL0.

Saturation Transfer EPR Spectra. The conventional V_1-EPR spectra (Figures 3 and 5) of the 5-MSL spin label indicate very little segmental mobility, for either membrane. Therefore, this label is likely to be suitable for studying the effects of the inhibitors on the overall rotational mobility of

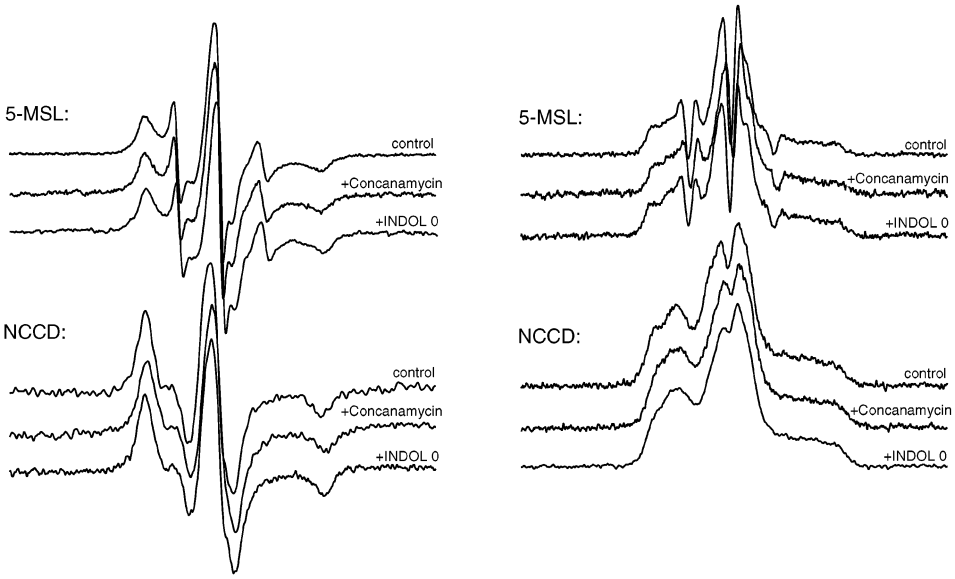

FIGURE 7: Saturation transfer EPR spectra (V_2'-display, at right) and conventional EPR spectra (V_1-display, at left) of *Nephrops* 16-kDa membranes covalently spin-labeled with 5-MSL (top panels) and NCCD (bottom panels). In each set of three spectra: (top spectrum) control sample, to which DMSO was added, (middle) sample containing concanamycin A, (bottom) sample containing INDOL0. The temperature was 5 °C; the total scan width was 160 G.

Table 1: Low- and High-Field ST-EPR Line Height Ratios, L″/L and H″/H, of *Nephrops* 16-kDa Membranes and Yeast Vacuolar Membranes Spin-Labeled with 5-MSL, in the Presence and Absence of V-ATPase Inhibitors[a]

L″/L			H″/H		
control	with concA[b]	with INDOL0	control	with concA[b]	with INDOL0
Nephrops 16-kDa					
1.25 ± 0.07 (120 ± 25)	1.32 ± 0.11 (145 ± 50)	1.42 ± 0.06 (200 ± 40)	1.02 ± 0.09 (145 ± 30)	1.13 ± 0.16 (180 ± 60)	1.43 ± 0.09 (345 ± 70)
Yeast Vacuole					
1.13 ± 0.05 (90 ± 10)	1.28 ± 0.06 (130 ± 20)	1.51 ± 0.03 (275 ± 30)	1.05 ± 0.14 (155 ± 50)	1.19 ± 0.15 (210 ± 65)	1.51 ± 0.07 (400 ± 65)

[a] $T = 5$ °C; diagnostic ST-EPR line heights are defined in ref *28*. Values of effective rotational correlation times (in microseconds), deduced from calibrations in ref *23*, are given in parentheses. [b] Concanamycin A.

the whole spin-labeled proteolipid assembly (see, for example, ref *27*). Figure 7 (top panel on the right) shows the V_2' ST-EPR spectra of *Nephrops* 16-kDa membranes spin-labeled with 5-MSL. Spectra were recorded at 5 °C to reduce the effects of residual segmental motion (see conventional spectra on the left of Figure 7). The ST-EPR spectrum from control membranes evidences slow but significant rotational mobility on the microsecond time scale, as is expected for overall motion of the transmembrane proteolipid assembly. Addition of concanamycin A does not change the ST-EPR line shape greatly. The indolyl inhibitor INDOL0, however, does change the line shape in the direction of decreasing rotational mobility.

Table 1 gives the diagnostic ST-EPR line height ratios, L″/L and H″/H, for the low- and high-field regions of the spectrum, respectively. Increasing line height ratio represents increasing intensity in the intermediate regions of the ST-EPR spectrum that are most sensitive to rotational motion, and implies a decreasing rate of rotational diffusion (*28*). For *Nephrops* 16-kDa membranes, a slight increase in ST-EPR line height ratio is induced by concanamycin A. INDOL0, however, causes a larger decrease in rotational mobility, as seen from the considerable increase in the ST-EPR line height ratios.

Effective isotropic rotational correlation times, τ_R^{eff}, deduced from the ST-EPR line height ratios by using calibrations from ref *23* are given in parentheses in Table 1. These effective values for control membranes are approximately 10-fold greater than the uniaxial rotational correlation time $\tau_{R,||}$ ($\sim$14 μs) that is predicted for a 16-kDa proteolipid hexamer [which has a diameter of ca. 6.8 nm (*5*)] in a membrane with a viscosity of 5 P (see ref *29*). The effective isotropic correlation time depends on the orientation, θ, of the nitroxide *z*-axis to the rotation axis according to the relationship $\tau_{R,||} = (\tau_R^{eff}/2)\sin^2\theta$ (see ref *27*). The measured effective correlation times would therefore be consistent with a tilt angle of $\theta \sim 26-29°$ of the spin label relative to the membrane normal. Concanamycin has a tendency to decrease the rotational mobility of the 16-kDa proteolipid (by ca. 20−25%). The synthetic inhibitor INDOL0 restricts the rotational diffusion more markedly; the correlation time is almost doubled on addition of an equivalent molar concentration of INDOL0. Possible sources for the decrease in apparent overall rotational mobility are an enhancement in protein−protein interactions, an increase in the effective membrane viscosity, and a conformational change that reduces the tilt angle, θ.

The bottom panel on the right of Figure 7 shows the corresponding V_2' ST-EPR spectra of *Nephrops* 16-kDa membranes spin-labeled with NCCD. Spectra in both the presence and absence of inhibitors evidence very low mobility. The effects of the inhibitors are seen in the center of the ST-EPR spectrum, but hardly at all in the outer wings. This suggests that the *z*-axis of the NCCD spin-label is

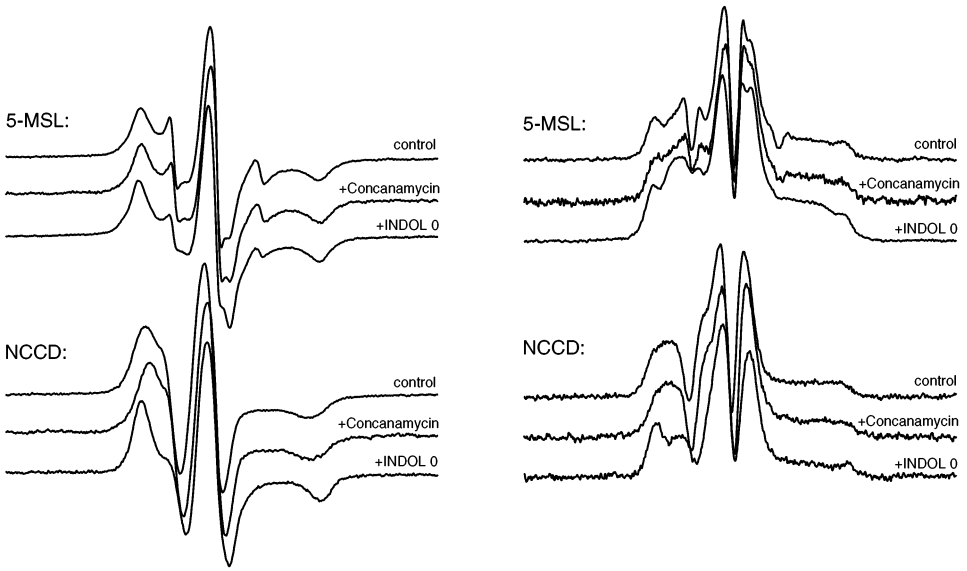

FIGURE 8: Saturation transfer EPR spectra (V_2'-display, at right) and conventional EPR spectra (V_1-display, at left) of yeast vacuolar membranes covalently spin-labeled with 5-MSL (top panels) and NCCD (bottom panels). In each set of three spectra: (top spectrum) control sample, to which DMSO was added, (middle) sample containing concanamycin A, and (bottom) sample containing INDOL0. The temperature was 5 °C; the total scan width was 160 G.

oriented almost perpendicular to the rotation axis, which causes the low-field and high-field regions of the ST-EPR spectrum to be insensitive to uniaxial rotation about the membrane normal (see ref *30*). Unlike with the 5-MSL spin label, the ST-EPR spectra of 16-kDa membranes labeled with NCCD are uncontaminated by a sharp, mobile spectral component. In this case, therefore, effective correlation times can be estimated from the C′/C diagnostic line height ratio that is defined in the central region of the ST-EPR spectrum. The effective values are: $\tau_R^{eff} = 95 \pm 5$ μs for control membranes, and $\tau_R^{eff} = 220 \pm 35$ and 520 ± 100 μs for membranes in the presence of concanamycin A and INDOL0, respectively. The relative effects of the inhibitors on overall rotational diffusion of the 16-kDa protein are in agreement with those deduced from the 5-MSL spin-label, which has a different orientation to the rotation axis. This suggests, therefore, that the decrease in mobility arises from protein−protein interactions, possibly augmented by a direct effect on the membrane lipid, rather than by a conformational change that affects the orientation θ.

The V_2' ST-EPR spectra of yeast vacuolar membranes spin-labeled with 5-MSL are shown in the top panel on the right of Figure 8. Qualitatively, they resemble those of 5-MSL-labeled *Nephrops* 16-kDa membranes, similarly at 5 °C. The diagnostic ST-EPR line height ratios and effective rotational correlation times for 5-MSL-labeled vacuolar membranes are also given in Table 1. Again, the pattern of perturbation of protein mobility by the inhibitors is similar to that found with 5-MSL-labeled *Nephrops* 16-kDa membranes. Concanamycin induces moderate increases in ST-EPR line height ratios and effective correlation times, whereas the INDOL0 inhibitor more than doubles the effective correlation time. In general terms, the effective rotational correlation times for vacuolar membranes are in ranges similar to those for the 16-kDa proteolipid. For the V-ATPase, a tightening of the interactions between the rotor (*c*, *c*′, and *c*″) and stator (*a*) units (see Figure 1) could give rise to decreased rotational mobility.

The bottom panel on the right of Figure 8 shows the V_2' ST-EPR spectra of vacuolar membranes spin-labeled with NCCD. In control membranes and those containing concanamycin A, the ST-EPR spectra at low field consist of a broad hump, without resolution between the diagnostic (i.e., L″-) and turning point (i.e., L-) regions. This feature originates from partial motional narrowing in the conventional V_1-EPR spectra that arises from segmental mobility (see the bottom panel on the left of Figure 8). It is then not possible to deduce meaningful effective rotational correlation times. In the presence of the INDOL0 inhibitor, segmental mobility of NCCD is largely suppressed (see the bottom left of Figure 8). Effective rotational correlation times are then 35 and 130 μs, deduced from the low-field and high-field line height ratios, respectively. Comparison of both the conventional EPR and ST-EPR spectra from NCCD-labeled samples containing INDOL0 in Figures 7 and 8 suggests that these lower effective correlation times in vacuolar membranes, relative to those in *Nephrops* 16-kDa membranes, most probably arise from residual segmental motion. A possible reason for this difference might be some heterogeneity of spin labeling in vacuolar membranes.

Mutational Analysis of Inhibitor Interaction. The biophysical data indicate that INDOL0 and concanamycin A act in a similar way, on the external lipid-facing regions of the 16-kDa proteolipid. A previous study has shown that mutations in this proteolipid from *Neurospora crassa* give rise to resistance to bafilomycin and partially to concanamycin A (*14*). All three mutations are in highly conserved transmembrane segments and may have partial lipid exposure (*7*). Two of these mutations are in the fourth transmembrane segment, on either side of the essential glutamic acid residue that reacts with DCCD. The similarities in the mode of action of concanamycin A and INDOL0 suggest that the same mutations should give rise to some resistance against both inhibitors.

To test the above, equivalent mutations, F135L and Y142H, were introduced into the *S. cerevisiae* form of the

Table 2: ATPase Activity of Vacuolar Membranes Isolated from Vatc Cells Expressing the Wild-Type or Mutant 16-kDa Proteolipid[a]

strain	no inhibitor	concanamycin A	INDOL0	DCCD
Vatc with wild-type HA1	0.140 ± 0.009	0.060 ± 0.002	0.050 ± 0.003	0.010 ± 0.002
Vatc with F135L HA1	0.100 ± 0.003	0.080 ± 0.005	0.070 ± 0.007	0.030 ± 0.002
Vatc with Y142H HA1	0.133 ± 0.006	0.100 ± 0.005	0.060 ± 0.013	0.020 ± 0.010
Vatc with an empty vector	0.008 ± 0.0008	0.008 ± 0.0003	0.008 ± 0.0003	0.007 ± 0.0006

[a] ATPase activity is shown as micromoles of P_i released per minute per milligram of protein. Final inhibitor concentrations are as follows: 25 nM concanamycin A, 1 μM INDOL0, and 0.2 mM DCCD.

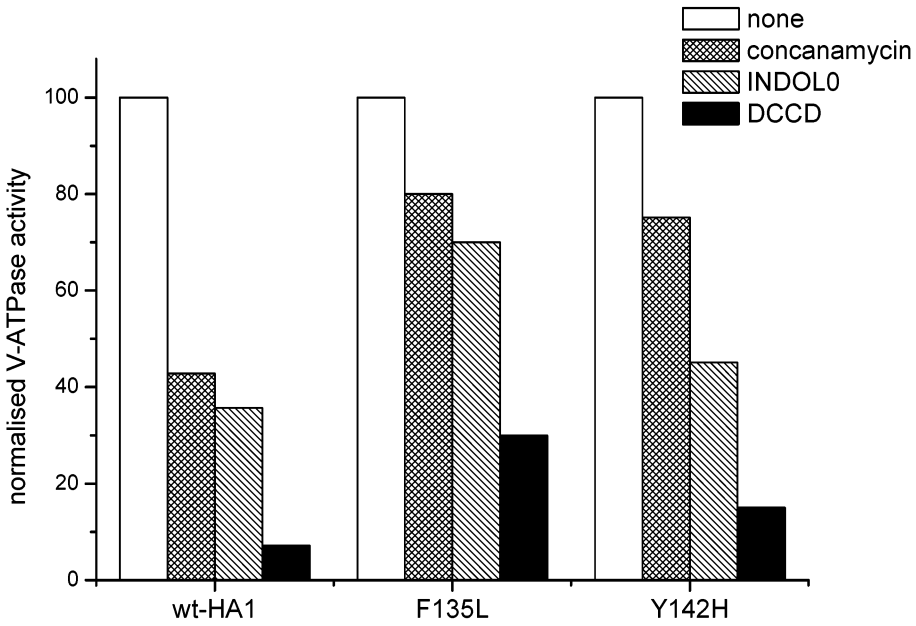

FIGURE 9: Inhibitor profile of ATPase activity in yeast vacuolar membranes expressing the wild-type or mutant *S. cerevisiae* 16-kDa proteolipid. Activity is shown as the percentage of that in the absence of inhibitors.

16-kDa proteolipid and expressed in the VMA3 null mutant (W303-b vatc) of *S. cerevisiae.* (The corresponding residues in the *Nephrops* 16-kDa proteolipid are F138 and Y145.) Vatc cells lack the proteolipid and do not assemble the V-ATPase, giving rise to the *vma* phenotype of conditional lethality that allows growth at pH 5.5 but not at neutral pH or at high extracellular calcium concentration. The mutant and control wild-type 16-kDa proteolipids were tagged at their C-termini with an HA1 epitope. All three rescue the VMA phenotype in vatc cells, giving growth of the vatc cells at pH 7.5 and in high extracellular calcium (data not shown). Table 2 and Figure 9 show inhibitor profiles of the ATPase activity in vacuolar membranes. As expected, the ATPase activity in vacuoles isolated from vatc cells expressing either the wild-type or the mutant 16-kDa proteolipid is inhibited to ≥75% by covalent modification with DCCD. However, the resistance to concanamycin A and INDOL0 is increased considerably in the F135L mutant compared to that in the wild-type control ($p < 0.005$ for concanamycin A and $p < 0.001$ for INDOL0), indicating a common binding site.

Interestingly, the degree of resistance to INDOL0 conferred by the Y142H mutation is smaller than that to concanamycin A, at concentrations that inhibit the wild-type proteolipid to comparable extents ($p < 0.5$ for INDOL0 and $p < 0.001$ for concanamycin A). This could indicate overlapping, but not necessarily totally identical, binding sites for the two inhibitors. There are parallels with the spin-label data, in that INDOL0 mostly induces greater immobilization than does concanamycin, particularly of the NCCD-labeled essential glutamate in vacuolar membranes. The yeast mutations also give rise to resistance to bafilomycin, to an even greater extent than to concanamycin.

CONCLUSIONS

The specifically spin-labeled residues C54 and E140 of the *Nephrops* 16-kDa proteolipid are situated on transmembrane segments 2 and 4, respectively, of the putative transmembrane four-helix bundle (*7*, *31*). On SDS gels, the V-ATPase is the principal protein of EDTA-washed yeast vacuolar membranes. Because substitution of the wild-type proteolipid by a polypeptide carrying an E140G mutation results in an approximately 90% decrease in vacuolar membrane protein labeling with a fluorescent carbodiimide analogue (*26*), we can be confident that this is the main site of labeling by DCCD. The sites that are selectively labeled by 5-MSL and NCCD in the 16-kDa proteolipid are therefore expected to make a major contribution to the EPR spectrum from the vacuolar membrane. Reaction with maleimide knocks out the ATPase activity in vacuolar membranes, but also probably labels other membrane-domain cysteines.

The effects of the INDOL0 inhibitor on the conventional EPR spectra of 5-MSL-labeled membranes are consistently greater, at equivalent nominal molar concentrations, than those of concanamycin A. This difference might not arise solely from intrinsically larger perturbations by INDOL0. There are possibly also differences in the degree of incorporation into the membrane, for the two inhibitors. The relatively large decreases in segmental mobility induced by INDOL0 suggest a direct interaction with both spin-labeled

residues, although effects of a conformational change cannot be excluded. In the model of the 16-kDa proteolipid of Harrison et al. (*31*) that is based on cysteine replacement mutagenesis and cross-linking (cf. Figure 1), residues C54 and E140 are situated in close proximity on adjacent helices that are accessible from the lipid bilayer milieu. This is consistent with both residues being involved in, or close to, the inhibitor binding site. Although the perturbations of segmental mobility are smaller in certain cases, the results with concanamycin A are also consistent with this interpretation. Both bafilomycin (*14*) and concanamycin (*25*) have been found to interact with the proteolipid *c* subunit. It is worth noting that in vertebrate tissues, the presence of specific subunit *a* isoforms (see Figure 1) confers differential sensitivity to these inhibitors, implying that additional interaction with subunit *a* may also be important (*32*, *33*).

The large reduction in the rotational mobility of the hexameric 16-kDa proteolipid assembly by INDOL0 suggests a potential mechanism of inhibitory action. It is possible that this inhibitor may interrupt the ATP-driven rotation of the proteolipid assembly that powers proton transport, as does concanamycin (*34*). The similar effects that concanamycin has on the ST-EPR spectra support this interpretation for INDOL0, and the mutational analysis supports a common binding site and mode of action for both classes of inhibitors.

ACKNOWLEDGMENT

We thank Frau B. Freyberg for excellent technical assistance, Frau B. Angerstein for synthesis of the NCCD spin-label, and Mrs. M. Scott for the preparation of *Nephrops* membranes. T.P., J.B.C.F., and D.M. are members of the COST D22 Action of the European Union.

REFERENCES

1. Nishi, T., and Forgac, M. (2002) The vacuolar H^+-ATPases: nature's most versatile proton pumps, *Nat. Rev. Mol. Cell. Biol. 3*, 94−103.
2. Sun-Wada, G. H., Wada, Y., and Futai, M. (2003) Vacuolar H^+ pumping ATPases in luminal acidic organelles and extracellular compartments: common rotational mechanism and diverse physiological roles, *J. Bioenerg. Biomembr. 35*, 347−358.
3. Holzenburg, A., Jones, P. C., Franklin, T., Páli, T., Heimburg, T., Marsh, D., Findlay, J. B. C., and Finbow, M. E. (1993) Evidence for a common structure for a class of membrane channels, *Eur. J. Biochem. 213*, 21−30.
4. Harrison, M. A., Jones, P. C., Kim, Y. I., Finbow, M. E., and Findlay, J. B. C. (1994) Functional properties of a hybrid vacuolar H^+-ATPase in *Saccharomyces* cells expressing the *Nephrops* 16-kDa proteolipid, *Eur. J. Biochem. 221*, 111−120.
5. Páli, T., Finbow, M. E., Holzenburg, A., Findlay, J. B. C., and Marsh, D. (1995) Lipid−protein interactions and assembly of the 16-kDa channel polypeptide from *Nephrops norvegicus*. Studies with spin-label electron spin resonance spectroscopy and electron microscopy, *Biochemistry 34*, 9211−9218.
6. John, S. A., Saner, D., Pitts, J. D., Holzenburg, A., Finbow, M. E., and Lal, R. (1997) Atomic force microscopy of arthropod gap junctions, *J. Struct. Biol. 120*, 22−31.
7. Páli, T., Finbow, M. E., and Marsh, D. (1999) Membrane assembly of the 16-kDa proteolipid channel from *Nephrops norvegicus* studied by relaxation enhancements in spin-label ESR, *Biochemistry 38*, 14311−14319.
8. Bowman, E. J., Siebers, A., and Altendorf, K. (1988) Bafilomycins: a class of inhibitors of membrane ATPases from microorganisms, animal cells and plant cells, *Proc. Natl. Acad. Sci. U.S.A. 85*, 7972−7976.
9. Dröse, S., Bindseil, K. U., Bowman, E. J., Siebers, A., Zeeck, A., and Altendorf, K. (1993) Inhibitory effect of modified bafilomycins and concanamycins on P-type and V-type adenosine triphosphatases, *Biochemistry 32*, 3902−3906.
10. Gagliardi, S., Gatti, P. A., Belfiore, P., Zocchetti, A., Clarke, G. D., and Farina, C. (1998) Synthesis and structure activity relationships of bafilomycin A(1) derivatives as inhibitors of vacuolar H^+-ATPase, *J. Med. Chem. 41*, 1883−1893.
11. Dröse, S., Boddien, C., Gassel, M., Ingenhorst, G., Zeeck, A., and Altendorf, K. (2001) Semisynthetic derivatives of concanamycin A and C, as inhibitors of V- and P-type ATPases: structure−activity investigations and developments of photoaffinity probes, *Biochemistry 40*, 2816−2825.
12. Farina, C., Gagliardi, S., Nadler, G., Morvan, M., Parini, C., Belfiore, P., Visentin, L., and Gowen, M. (2001) Novel bone antiresorptive agents that selectively inhibit the osteoclast V-H^+-ATPase, *Farmaco 56*, 113−116.
13. Nadler, G., Morvan, M., Delimoge, I., Belfiore, P., Zocchetti, A., James, I., Zembryki, D., Lee-Rycakzewski, E., Parini, C., Consolandi, E., Gagliardi, S., and Farina, C. (1998) (2*Z*,4*E*)-5-(5,6-Dichloro-2-indolyl)-2-methoxy-*N*-(1,2,2,6,6-pentamethylpiperidin-4-yl)-2,4-pentadienamide, a novel, potent and selective inhibitor of the osteoclast V-ATPase, *Bioorg. Med. Chem. Lett. 8*, 3621−3626.
14. Bowman, B. J., and Bowman, E. J. (2002) Mutations in subunit c of the vacuolar ATPase confer resistance to bafilomycin and identify a conserved antibiotic binding site, *J. Biol. Chem. 277*, 3965−3972.
15. Azzi, A., Bragadin, M. A., Tamburro, A. M., and Santato, M. (1973) Site-directed spin-labeling of the mitochondrial membrane. Synthesis and utilization of the adenosine triphosphatase inhibitor (*N*-(2,2,6,6-tetramethyl-piperidyl-1-oxyl)-*N*′-(cyclohexyl)-carbodiimide), *J. Biol. Chem. 248*, 5520−5526.
16. Girvin, M. E., and Fillingame, R. H. (1994) Hairpin folding of subunit *c* of F_1F_o ATP synthase: ^1H distance measurements to nitroxide-derivatized aspartyl-61, *Biochemistry 33*, 665−674.
17. Hertzberg, E. L. (1984) A detergent-independent procedure for the isolation of gap junctions from rat liver, *J. Biol. Chem. 259*, 9936−9943.
18. Leitch, B., and Finbow, M. E. (1990) The gap junction-like form of a vacuolar proton channel component appears not to be an artifact of isolation: an immunocytochemical localization study, *Exp. Cell Res. 190*, 218−226.
19. Uchida, E., Ohsumi, Y., and Anraku, Y. (1985) Purification and properties of H^+-translocating, Mg^{2+}-adenosine triphosphatase from vacuolar membranes of *Saccharomyces cerevisiae*, *J. Biol. Chem. 260*, 1090−1095.
20. Fajer, P., and Marsh, D. (1982) Microwave and modulation field inhomogeneities and the effect of cavity Q in saturation transfer ESR spectra. Dependence on sample size, *J. Magn. Reson. 49*, 212−224.
21. Hemminga, M. A., De Jager, P. A., Marsh, D., and Fajer, P. (1984) Standard conditions for the measurement of saturation transfer ESR spectra, *J. Magn. Reson. 59*, 160−163.
22. Horváth, L. I., and Marsh, D. (1983) Analysis of multicomponent saturation transfer ESR spectra using the integral method: application to membrane systems, *J. Magn. Reson. 54*, 363−373.
23. Marsh, D. (1999) Spin label ESR spectroscopy and FTIR spectroscopy for structural/dynamic measurements on ion channels, *Methods Enzymol. 294*, 59−92.
24. Gibson, L., Cadwallader, G., and Finbow, M. E. (2002) Evidence that there are two copies of subunit c″ in V_0 complexes in the vacuolar H^+-ATPase, *Biochem. J. 366*, 911−919.
25. Huss, M., Ingenhorst, G., König, S., Gassel, M., Dröse, S., Zeeck, A., Altendorf, K., and Wieczorek, H. (2002) Concanamycin A, the specific inhibitor of V-ATPases, binds to the V_o subunit c, *J. Biol. Chem. 277*, 40544−40548.
26. Harrison, M., Powell, B., Finbow, M. E., and Findlay, J. B. C. (2000) Identification of lipid-accessible sites on the *Nephrops* 16-kDa proteolipid incorporated into a hybrid vacuolar H^+-ATPase: Site-directed labeling with *N*-(1-pyrenyl)cyclohexylcarbodiimide and fluorescence quenching analysis, *Biochemistry 39*, 7531−7537.
27. Marsh, D., and Horváth, L. I. (1989) Spin-label studies of the structure and dynamics of lipids and proteins in membranes, in *Advanced EPR. Applications in Biology and Biochemistry* (Hoff, A. J., Ed.) pp 707−752, Elsevier, Amsterdam.
28. Thomas, D. D., Dalton, L. R., and Hyde, J. S. (1976) Rotational diffusion studied by passage saturation transfer electron paramagnetic resonance, *J. Chem. Phys. 65*, 3006−3024.

29. Cherry, R. J., and Godfrey, R. E. (1981) Anisotropic rotation of bacteriorhodopsin in lipid membranes, *Biophys. J. 36*, 257−276.
30. Marsh, D. (1980) Molecular motion in phospholipid bilayers in the gel phase: long axis rotation, *Biochemistry 19*, 1632−1637.
31. Harrison, M. A., Murray, J., Powell, B., Kim, Y. I., Finbow, M. E., and Findlay, J. B. C. (1999) Helical interactions and membrane disposition of the 16-kDa proteolipid subunit of the vacuolar H^+-ATPase analyzed by cysteine replacement mutagenesis, *J. Biol. Chem. 274*, 25461−25470.
32. Zhang, J. M., Feng, Y., and Forgac, M. (1994) Proton conduction and bafilomycin binding by the V_0 domain of the coated vesicle V-ATPase, *J. Biol. Chem. 269*, 23518−23523.
33. Gagliardi, S., Nadler, G., Consolandi, E., Parini, C., Morvan, M., Legave, M. N., Belfiore, P., Zocchetti, A., Clarke, G. D., James, I., Nambi, P., Gowen, M., and Farina, C. (1998) 5-(5,6-Dichloro-2-indolyl)-2-methoxy-2,4-pentadienamides: novel and selective inhibitors of the vacuolar H^+-ATPase of osteoclasts with bone antiresorptive activity, *J. Med. Chem. 41*, 1568−1573.
34. Hirata, T., Iwamoto-Kihara, A., Sun-Wada, G. H., Okajima, T., Wada, Y., and Futai, M. (2003) Subunit rotation of vacuolar-type proton pumping ATPase, *J. Biol. Chem. 278*, 23714−23719.

BI0493867